Surface plasmon-enhanced Raman scattering at thin silver films

Robert M. Corn and Michael R. Philpott

IBM Research Laboratory, San Jose, California 95193

Raman spectra are reported for liquids and Langmuir films enhanced by the electromagnetic fields of plasmon surface polaritons at flat silver surfaces. The Kretschmann prism coupling configuration is used to excite the incident surface polariton and to couple out the Raman shifted surface wave. The spectra are interpreted with the help of a simple quantum theory and compared with previously reported grating spectra. Enhancement factors, polarization characteristics, and the feasibility of using surface polaritons to enhance the Raman spectra of adsorbates on flat electrodes in contact with aqueous electrolyte are discussed.

This note reports the generation of Raman shifted plasmon surface polaritons (PSPs) in liquids and Langmuir monolayer assemblies adjacent to thin films of metallic silver. The PSPs enhance the Raman scattering near the silver film by increasing the incident and scattered radiation fields at the metal surface. The work closest to that described here is due to Ushioda and Sasaki,[1] who have used the technique of attenuated total reflection (ATR) in the Kretschmann[2] configuration to obtain the Raman spectrum of methanol in the C–H stretching region. Our work extends their efforts by demonstrating the generality of the technique, applying it to other molecular liquids and different frequency regions. By the use of monolayer films prepared by the Langmuir Blodgett dipping method,[3] we further demonstrate that the technique is certainly applicable to thin layers of surface materials. The results are interpreted here with a simple quantized model for the radiation field. This model allow us to discuss selection rules and the separation of enhancement factors for the in-coupled and out-coupled radiation in a simple and concise manner.

Several groups have excited surface plasmon polaritons by prism techniques to enhance the Raman scattering near the metal surface.[4–6] However, these groups did not collect light scattered out through the surface polariton channel. Surface polaritons have been previously employed on gratings to obtain the Raman scattering from molecules near a metal surface.[7–10] In addition to spontaneous Raman scattering, surface plasmon enhancement of coherent anti-Stokes Raman scattering (CARS) has been obtained for benzene at a silver surface.[11] Theoretical discussions of the spontaneous Raman scattering and CARS mediated by surface plasmons using classical electromagnetic fields have occurred recently in the literature.[6,12–15] An upper bound on the field enhancement available from surface plasmons has been determined from energy considerations by Weber and Ford.[15] This work was undertaken to study the feasibility of using the enhancement from surface polaritons to obtain the Raman spectra of adsorbates on optically flat metal electrodes without the need for an oxidation-reduction cycle (ORC).

By using prism or grating couplers, it is possible to excite PSPs with almost unit efficiency. Likewise, it is possible to couple PSPs out from the surface with the same techniques. Consequently, the simplest model for surface polariton enhanced Raman scattering is one where we ignore the excitation and collection coupling problems and concentrate on the Raman scattering between two PSP channels. The essential physics involved is illustrated pictorially in Fig. 1. The inset shows the process of coplanar scattering, as represented on the dispersion curves with surface polaritons at the interface between a metal and a condensed phase (e.g., a liquid). The coupler excites a PSP at point A on the dispersion curve; the scattered light at the Stokes frequency is coupled out at point B. For prism couplers such as the Kretschmann configuration, there are actually two PSP branches, as noted in the inset to Fig. 1. However, the lower branch, localized mainly at the metal-prism interface, is not radiative and therefore the Raman scattering from point A to this branch cannot be detected even though it is energetically allowed.

Once the PSP at point A is created, the Raman scattering from the surface is not limited to the plane of incidence. Instead, the PSP at point B can propagate in any direction along the surface as long as it is permitted to do so by the elements of the Raman polarizability tensor. Thus, as depicted in the main portion of Fig. 1, the scattered light from an incident beam along the positive x axis will emerge from the prism coupler in a cone, whose angle with the surface will be governed by the dispersion relation shown in the inset. This is in contrast to coherent processes such as second harmonic generation or coherent anti-Stokes Raman scattering, whose output angle will be limited to that required by the phase-matching conditions of the nonlinear effect.

A simple quantum mechanical formulation of the radiative part of the Raman problem starts with the Hamiltonian for a single molecule located at a fixed distance $r = (0,0,z)$ above a plasma half-space ($z < 0$). The Hamiltonian for this model can be written as the sum of four parts:

$$H_{\text{TOT}} = H_{\text{mol}} + H_{\text{met}} + H_{\text{rad}} + H_{\text{int}}, \qquad (1)$$

where mol, met, rad, and int refer to the molecular, metal, radiation, and interaction parts of the Hamiltonian. We will assume that the metal will interact with the molecule only through its modification of H_{rad}, which in turn interacts with the molecule via H_{int}. In addition, only frequencies below the surface polariton cutoff frequency ω_{sp}, which is related to the plasma frequency ω_p of the metal by $\omega_{sp} = \omega_p (1 + \epsilon_a)^{1/2}$, will be considered. In the Coulomb gauge, the vector potential A of the quantized radiation field can be written as the sum of three vectors:

$$\mathbf{A} = \mathbf{A}_s + \mathbf{A}_p + \mathbf{A}_{sp}. \qquad (2)$$

Here $\mathbf{A}_s$ and $\mathbf{A}_p$ are the contributions from s- and p-polarized photons. Their contribution to the Raman scatter-
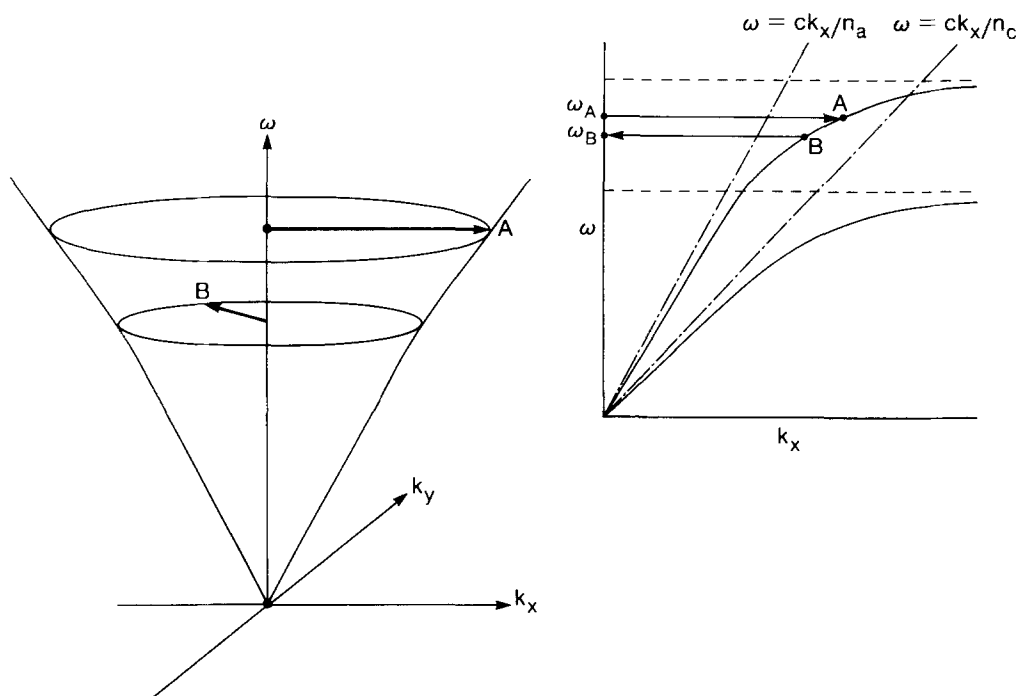
© 1984 American Institute of Physics 5245

FIG. 1. Raman scattering process on a surface via surface plasmon polaritons. The PSP A is injected onto the surface long the positive x axis; a Raman shifted PSP is created in the B direction. The dispersion relation for PSPs in the thin silver film-prism coupling system is depicted in the inset to Fig. 1; the upper curve represents PSPs which are coupled to ingoing and outgoing EM waves at the silver-prism interface. From this dispersion relation, we see that the scattering cone for **B** is at a different angle than the input cone for **A**.

ing is small as long as $z/\lambda \ll 1$, and it will be neglected in comparison to that from the third term $\mathbf{A}_{sp}$, which is due to the surface polaritons. This surface vector potential can be written as

$$\mathbf{A}_{sp}(z) = \sum_k \mathbf{A}_k(z) e^{ik\cdot\rho},\tag{3}$$

where

$$\mathbf{A}_k(z) = \left(\frac{4\pi\hbar c}{L^2 p_k}\right)^{1/2} (a_k + a^+_{-k})$$
$$\times \left[\theta(z)\left(i\hat{k} - \frac{k}{v_a}\hat{z}\right)e^{-v_a|z|}\right.$$
$$\left. + \theta(-z)\left(i\hat{k} + \frac{k}{v_b}\hat{z}\right)e^{-v_b|z|}\right]\tag{4}$$

with

$$p_k = \frac{\epsilon_b^4 - \epsilon_a^4}{\epsilon_a^2 \epsilon_b^2}\left[-(\epsilon_a + \epsilon_b)\right]^{-1/2}\tag{5}$$

and

$$v_i^2 = k^2 - \epsilon_i \omega_k^2/c^2, \quad i = a,b.\tag{6}$$

The letters a and b in Eqs. (4)–(6) refer to the dielectric and the metal respectively; all other symbols have their usual meaning. $\theta(z)$ is the Heavyside step function and a_k and a_k^+ are the annihilation and creation operators for a PSP of wave-vector **k**. This Hamiltonian is essentially that of Elson and Ritchie,[16,17] except that we assume that the dielectric constants are complex (i.e., there can be dissipation of the PSP in the final expressions for rates and cross sections). The dispersion relation for the frequency ω_k of the surface polariton with wave vector k along the surface is given by

$$\omega_k^2 = \frac{1}{2}\omega_p^2 + c^2 k^2 - \left(\frac{1}{4}\omega_p^4 + c^4 k^4\right)^{1/2}.\tag{7}$$

Equation (7) is only approximate since in this model we are looking at a single interface. The dispersion relation for the

film prism coupler arrangement actually employed in the experiments will reach this value as the thickness d of the thin film becomes large.[1]

The interaction betweeen the molecule, the metal, and the radiation field is carried by the vector potential according to

$$H_{\text{int}} = -\boldsymbol{\mu}\cdot\mathbf{E},\tag{8}$$

where $\boldsymbol{\mu}$ is the point dipole operator of the molecule and the electric field **E** is given by

$$\mathbf{E} = -\frac{1}{c}\dot{\mathbf{A}} = \sum_k\left(\frac{i\omega_k}{c}\right)\mathbf{A}_k(z)e^{ik\cdot\rho}.\tag{9}$$

To calculate the transition rate for Raman scattering, we assume that the initial and final states are the product of molecular and surface plasmon states:

$$|\Phi_i\rangle = |n_k\rangle|\phi_i\rangle,\tag{10}$$

$$|\Phi_f\rangle = |n_k - 1\rangle|n_{k'}\rangle|\phi_f\rangle,\tag{11}$$

where ϕ_i and ϕ_f are the molecular eigenstates, and n_k is the surface plasmon state with frequency ω_k and occupation number n_k. To second order the transition rate P_{fi} is given by the Fermi golden rule expression:

$$P_{fi} = \frac{2\pi}{\hbar}|M_{fi}|^2\delta(E_f - E_i),\tag{12}$$

where the second order scattering matrix element M_{fi} is given by

$$M_{fi} = -\frac{4\pi\hbar}{cL^2}(p_k p_k')^{-1/2} n_k^{1/2}\omega_k\omega_{k'}\cdot e^{-(v_a + v_a')z}$$
$$\times \mathbf{e}_k:\boldsymbol{\alpha}_{fi}:\mathbf{e}_{k'},\tag{13}$$

and we have defined $\mathbf{e}_k = i\hat{k} - k/v_a\hat{z}$. The second rank tensor $\boldsymbol{\alpha}$ is the standard Raman polarizability tensor for an oriented molecule. Off resonance, it has the form

$$\boldsymbol{\alpha} = \frac{1}{\hbar}\sum_v \frac{\langle\phi_f|\boldsymbol{\mu}|\phi_v\rangle\langle\phi_v|\boldsymbol{\mu}|\phi_i\rangle}{\omega_v - \omega_k},$$

$$+ \frac{\langle \phi_v | \boldsymbol{\mu} | \phi_i \rangle \langle \phi_f | \boldsymbol{\mu} | \phi_v \rangle}{\omega_v + \omega_k}, \tag{14}$$

where $\hbar\omega_v$ is the energy difference between ϕ_i and ϕ_v. Since Eq. (14) is only good to second order, there are no corrections for image dipole interactions, i.e., the energy levels of the virtual molecular states $\hbar\omega_v$ are not shifted or broadened by interaction with any part of the radiation field. Assuming unit conversion efficiency from photons to surface plasmons, the incident power flux S_p through the surface is given by

$$S_p = \hbar\omega_k n_k L^{-2} (\epsilon_0/\epsilon_a)^{1/2}. \tag{15}$$

From this power, an amount ΔP is scattered into the angle $d\theta$ at the Raman frequency

$$\Delta P_{d\theta} = \frac{8\pi\omega_k^2 \omega_{k'}^3}{\hbar c^2 L^2} n_k (p_k p_{k'})^{-1} e^{-2(v_a + v_a')z}$$

$$\times |\mathbf{e}_k : \boldsymbol{\alpha} : \mathbf{e}_{k'}|^2 k' \left| \frac{dk}{d\omega} \right|_{\omega_{k'}}, \tag{16}$$

where the density states term $k' |dk/d\omega|_{\omega_{k'}}$ can be obtained from the dispersion relation for the surface polaritons [Eq. (7)]. The ratio of Eqs. (15) and (16) yields the differential cross section for Raman scattering form surface polaritons:

$$\frac{d\sigma}{d\theta} = \frac{8\pi}{c^3} \left(\frac{\epsilon_a}{\epsilon_0} \right)^{1/2} (p_k p_{k'})^{-1} e^{-2(v_a + v_a')z}$$

$$\times |\mathbf{e}_k : \boldsymbol{\alpha} : \mathbf{e}_{k'}|^2 k' \left| \frac{dk}{d\omega} \right|_{\omega_{k'}}. \tag{17}$$

The differential Raman scattering cross section in Eq. (17) differs from Raman cross section for a bulk sample $d\sigma/d\Omega$:

$$\frac{d\sigma}{d\Omega} = \frac{1}{16\pi\epsilon_0^2 c^4} \left(\frac{\epsilon_a'}{\epsilon_a} \right)^{1/2} \omega_k^4 |\mathbf{e} : \boldsymbol{\alpha} : \mathbf{e}'|^2. \tag{18}$$

There are three aspects to the difference between Eqs. (17) and (18); each one contributes to the enhancement of the Raman signal. The first is the exponential term in Eq. (17) which localizes the Raman scattering to the surface. For the silver/n-hexane system, the Raman scattering cross section has dropped to $1/e$ of its value at the surface by 40 nm. We are, therefore, measuring the Raman scattering from a very small volume of material adjacent to the metal surface. The second aspect of the cross section for the Raman scattering process by surface polaritons is the density of states term $k' |dk/d\omega|_{\omega_{k'}}$ in Eq. (17). This term can become quite large since the density of states diverges at the surface plasmon cutoff frequency.[17] The final difference between $d\sigma/d\theta$ and $d\sigma/d\Omega$ is the units: $d\sigma/d\Omega$ has units of cm^2, $d\sigma/d\theta$ is in cm. The apparent discrepancy arises from the fact that the first case the scattering is into a volume, whereas in the second case the scattering is into a plane. This is just a manifestation of localization of the Raman scattering into the scattering cone depicted in Fig. 1.

The PSP modes at the interface are TM polarized; the actual direction of the polarization is given by the vector quantity $\mathbf{e}_k$. For the case of the metal-dielectric interface, the polarization is almost perpendicular to the surface since $k/v_a \approx (\epsilon_b/\epsilon_a)^{1/2} > 1$. However, there is some elliptical longitudinal polarization present. If we define the x axis to be along k, the direction of the incident polariton, then the Raman

cross section depends on the elements of the Raman polarizability tensor by Eq. (19):

$$\frac{d\sigma}{d\theta} \propto \left| \frac{kk'}{v_a v_a'} \alpha_{zz} \right.$$

$$+ i \left[\frac{k}{v_a} (\alpha_{xz} \cos\theta + \alpha_{yz} \sin\theta) + \frac{k'}{v_a'} \alpha_{zx} \right] \tag{19}$$

$$- (\alpha_{xx} \cos\theta + \alpha_{yx} \sin\theta) \bigg|^2.$$

If, to first order, we neglect the $i\hat{k}$ term in $\mathbf{e}_k$ (implying that the incident and "collected" light are polarized perpendicular to the scattering plane) then for an oriented molecule the Raman cross section is dependent only on α_{zz}, the zz component of the Raman polarizability tensor:

$$\frac{d\sigma}{d\theta} \propto |\alpha_{zz}|^2. \tag{20}$$

This cross section is independent of the angle in the scattering plane. Thus, to first order the Raman scattering intensity is independent of position on the scattering cone in Fig. 1. Note that α_{zz} refers to space-fixed axes, not molecular axes, so that for oriented molecules α_{zz} is given in terms of molecular polarizabilities[18]:

$$\alpha_{zz} = \sum_{gg'} \Phi_{zg} \Phi_{zg'} \alpha_{gg'}, \tag{21}$$

where Φ_{zg} and $\Phi_{zg'}$ are the direction cosines between the space fixed z axis and the molecular $(g = x, y, z)$ axes. Thus, the Raman spectrum obtained from the PSPs will give us direct information concerning the orientation of the molecules near the surface.

For a collection of randomly oriented molecules, such as in a liquid, we must average over the direction cosines in Eq. (21), yielding the standard result

$$\frac{d\sigma}{d\theta} \propto \frac{45a^2 + 4\gamma^2}{45}, \tag{22}$$

where a and γ are the spherical and anisotropic parts of the molecular Raman tensor. From Eq. (22), we see that the Raman spectrum from PSPs at the metal interface should be directly comparable to the H–H Raman scattering spectrum $[I_\parallel (\text{obs. } \perp)$ in the notation of Ref. 18] from the bulk liquid.

A schematic of the prism, silver film, and the cell is shown in Fig. 2. The cell was designed for use in electrochemistry, having ports for reference and counter electrodes. Silver films of a thickness of 45 nm were vapor deposited onto the flat side of a hemicylindrical prism made of Schott LASF5 glass (refractive index = 1.89 at λ = 530.9 nm). Figure 3 shows a rough schematic of the experiment. The sample cell and prism were rotated on a specially constructed table until the p-polarized incident laser light excited the PSP at the metal-sample interface. The scattering angle was then independently selected to correspond to the plasmon angle of the PSP at the wavelength of the Stoke's shifted light for the sample (the C–H stretching region in the case of n-hexane and the Langmuir deposited films and the C–Cl stretch in the case of CCl$_4$). Both the input and output angles were calculated using Fresnel's equations and the tabulated complex values of the dielectric constant for silver.[19] The calculations agreed with the experimentally measured values to within 1°. The Raman spectra were recorded with a Spex 14018 double monochromator with all silver optics and
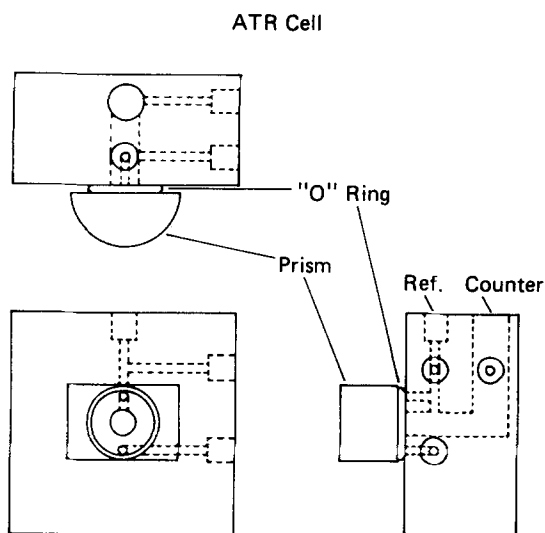
ATR Cell

FIG. 2. ATR cell for the liquid experiments. The liquid is contained by the O ring which seals the prism to the cell. Various ports for electrochemical measurements were included in the cell for future experiments.

conventional computerized signal gathering and averaging capabilities.

The Raman spectra of the C–H stretching region of n-hexane and the C–Cl stretching region of CCl₄ generated from PSPs near a thin silver film are shown in Figs. 4 and 5. The incident laser light from a Kr⁺ laser ($\lambda = 530.9$ nm) was injected into a PSP using an angle of incidence of 53.5° inside the LASF5 prism for the n-hexane sample ($\eta_c = 1.37$) and at 59.5° for the CCl₄ sample ($\eta_c = 1.46$). Also shown in each figure is the H–H spectrum recorded from the bulk liquid. The spectra are virtually identical (as required by theory) except for some possible broadening of the hexane band due to the antisymmetric methyl stretch at 2965 cm⁻¹. This band is known to be very sensitive to intermolecular effects.[20] The spectra in Figs. 4 and 5 were recorded at the
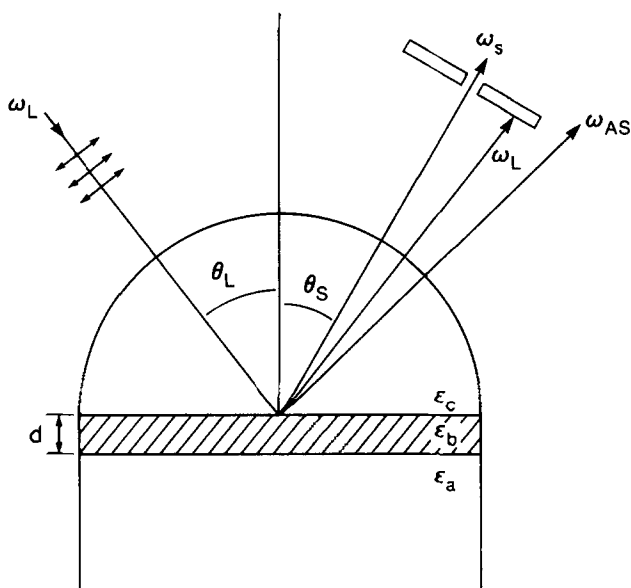

FIG. 3. Schematic diagram of the experimental setup.The sample was mounted on a rotary table which allowed the independent selection of θ_1 and θ_s. A slit was placed in front of the spectrometer in order to reject the residual reflected laser light. The prism material was LASF5 ($\eta = 1.89$ at 530.9 nm) and the silver film thickness was 45 nm.
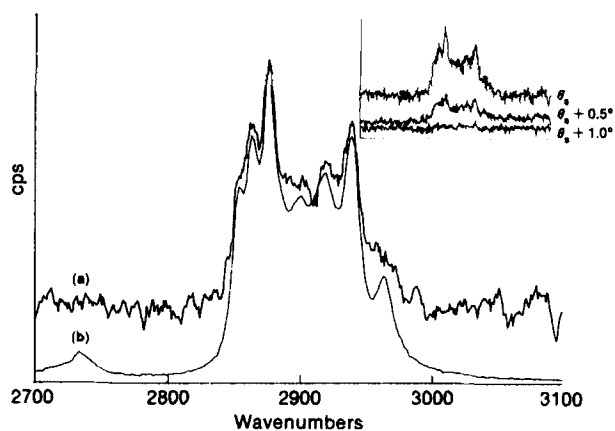

FIG. 4. Curve (a): PSP-enhanced spectra of the CH stretching region of n-hexane at a thin silver film (45 nm). For comparison, the liquid H–H Raman scattering spectrum is also shown [curve (b)]. The laser excitation frequency was 530.9 nm, laser power 50 mW. Input angle $\theta_1 = 53.5°$, output angle $\theta_s = 52°$. As shown in the inset, no spectrum was observed 1° off the output angle for the PSP.

scattering angle for the PSP at the Stokes wavelength (51.6° for n-hexane and 59.5° for CCl₄). As shown in the inset to Fig. 4, no signal was detected beyond 1° off of this angle.

As another example of this technique, Fig. 6 shows the PSP enhanced Raman spectra of ten monolayers of cadmium arachidate laid down by Langmuir–Blodgett dipping methods. The film was deposited by dipping the silver coated prism directly into the Langmuir tank. For comparison, the inset in the figure shows the Raman spectrum of 28 arachidate layers deposited onto a silver grating with groove depth of 10 nm and groove spacing of 400 nm.[9] Both the theory and the liquid experiments indicate that we are measuring only α_{zz} with the PSP enhanced Raman spectrum at the flat surface, so that this spectrum provides the best method (along with the infrared spectrum) for determining the molecular orientation of Langmuir films. In addition to monolayers, this technique should prove to be quite useful in studying the orientation of thin polymer films, and to molecular orientations in liquid crystals. Some further work along these general lines is planned.
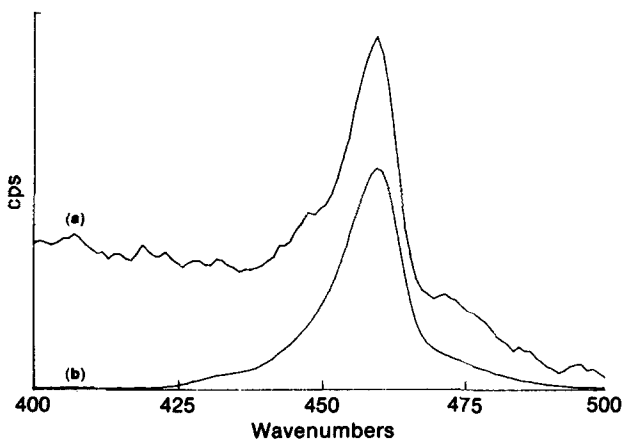

FIG. 5. Curve (a): PSP-enhanced spectra of the C–Cl stretching region of CCl₄ at a thin silver film. Same parameters as in Fig. 4, except that $\theta_1 = 59.5°$ and $\theta_s = 59°$. As in Fig. 4, the liquid spectrum is shown from comparison [curve (b)].
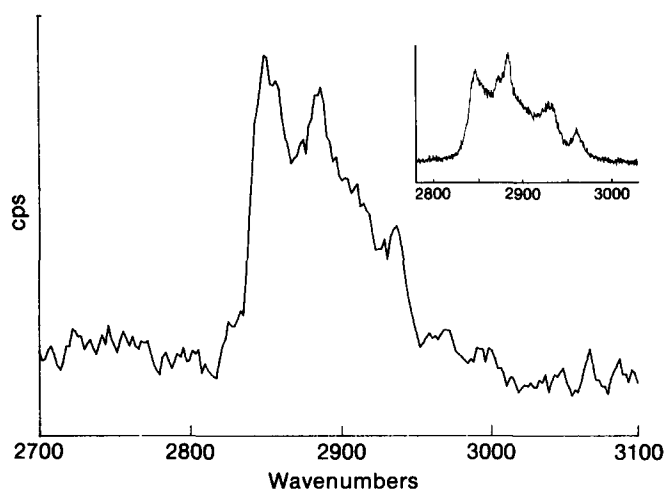
FIG. 6. PSP-enhanced spectra of the CH stretching region of ten monolayers of cadmium arachidate at a thin silver film. Depicted in the inset for comparison is the Raman spectra from 28 monolayers deposited onto a silver grating (inset spectrum taken from Ref. 9).

As a final note, we would like to mention the possibility of utilizing PSP enhanced Raman spectroscopy at optically flat electrodes. The technique of surface enhanced Raman spectroscopy (SERS) has been extensively used to detect the presence of adsorbates on silver, copper, and gold electrodes after the latter have been subjected to an ORC.[21] The process of electrode activation results in a rough surface on which there are sites responsible for most if not all of the observed Raman signal. The Raman enhancement is believed to arise from a combination of electromagnetic field enhancement due to localized surface plasma resonances associated with particulate-like surface structures and a chemical factor from the structure of the molecular site.[22] Since the active sites occupy a minority of the surface (0.1% to 0.3%)[23] the ability of SERS to study the majority species on the surface is indirect and very limited at best. The use of enhancements due to PSPs on flat surfaces to record the Raman spectra of adsorbates would remove the limitations presently inherent in current SERS techniques and would make the phenomenon of surface enhanced Raman a genuinely useful tool for the study of the aqueous electrolyte interface at silver, copper, and gold electrodes.

[1]S. Ushioda and Y. Sasaki, Phys. Rev. B **27**, 1401 (1982).
[2]E. Kretschmann and H. Raether, Z. Naturforsch. Teil A **23**, 2135 (1968).
[3]H. Kuhn, D. Mobius, and H. Bucher, in *Physical Methods of Chemistry*, edited by A. Weissberger and B. W. Rossiter (Wiley, New York, 1972), Part III B, Chap. VII.
[4]B. Pettinger, A. Tadjeddine, and D. M. Kolb, Chem. Phys. Lett. **66**, 544 (1979).
[5]R. Dornhaus, R. E. Benner, R. K. Chang, and I. Chabay, Surf. Sci. **101**, 367 (1980).
[6]See, for example, the review papers in *Surface Polaritons*, edited by V. M. Agranovich and D. L. Mills (North–Holland, Amsterdam, 1982).
[7]A. Girlando, J. G. Gordon II, D. Heitmann, M. R. Philpott, H. Seki, and J. D. Swalen, Surf. Sci. **101**, 417 (1980).
[8]A. Girlando, M. R. Philpott, D. Heitmann, J. D. Swalen, and R. Santo, J. Chem. Phys. **72**, 5187 (1980).
[9]W. Knoll, M. R. Philpott, J. D. Swalen, and A. Girlando, J. Chem. Phys. **72**, 2254 (1982).
[10]J. C. Tsang, J. R. Kirtley, and J. A. Bradley, Phys. Rev. Lett. **43**, 772 (1979).
[11]C. K. Chen, A. R. B. De Castro, Y. R. Shen, and F. DeMartini, Phys. Rev. Lett. **43**, 946 (1979).
[12]Y. J. Chen, W. P. Chen, and E. Burstein, Phys. Rev. Lett. **36**, 1207 (1976).
[13]S. S. Jha, J. R. Kirtley, and J.C. Tsang, Phys. Rev. Lett. **22**, 3973 (1980).
[14]K. Sakoda, K. Ohtaka, and E. Hanamura, Solid State Commun. **41**, 393 (1982).
[15]W. H. Weber and G. W. Ford, Opt. Lett. **6**, 122 (1981).
[16]J. M. Elson and R. H. Richie, Phys.Rev. B **4**, 4129 (1971).
[17]M. R. Philpott, J. Chem. Phys. **62**, 1812 (1975).
[18]E. B. Wilson, J. C. Decius, and P.C. Cross, *Molecular Vibrations* (Dover, New York, 1980).
[19]P. B. Johnson and R. W. Christy, Phys.Rev. B **6**, 4270 (1972).
[20]R. A. MacPhail, R. G. Snyder, and H. L. Strauss, J. Chem. Phys. **77**, 1118 (1982).
[21]R. P. Van Duyne, in *Chemical and Biochemical Applications of Lasers*, edited by C. B. Moore (Academic, New York, 1978), Vol. 4, p. 101.
[22]A. Otto, in *Light Scattering in Solids*, edited by M. Cardona and G. Guntherodt (Springer, Berlin, 1983), Vol. 4.
[23]B. Pettinger and L. Moerl, J. Electron Spectrosc. Relat. Phenom. **29**, 383 (1983).